*31st EPS Conference on Plasma Phys. London, 28 June - 2 July 2004 ECA Vol.**28G**, P-1.166 (2004)*

Modeling of Resistive Wall Mode Experiments in JET

Y.Q. Liu[1], T.C. Hender[2], M. Gryaznevich[2], D.F. Howell[2],
S.D. Pinches[3], R.J. Buttery[2], A. Bondeson[1] and JET EFDA contributors[4]

[1]*Department of Electromagnetics, EURATOM/VR Fusion Association*
Chalmers University of Technology, Göteborg, Sweden
[2]*EURATOM/UKAEA Fusion Association, Culham Science Centre, Abingdon, UK*
[3]*Max-Plank Institute for Plasmaphysik, EURATOM-Assoziation, Garching, Germany*
[4]*Annex J Paméla et al, Fusion Energy 2002, Proc 19th IAEA Fus Energy Conf, Lyon 2002*

1. Introduction

Advanced tokamaks have favorable micro-instabilities and thereby good transport properties, but the operational space (in terms of achievable pressure limits) is limited by ideal external kink modes, with low toroidal mode numbers $n = 1, 2, 3$. A conducting wall suppresses the instability at the resistive decay time of the wall eddy currents. At longer time scale, the stabilization is lost and the resulting slowly growing mode is called resistive wall mode (RWM). The RWM needs to be stabilized in order to achieve steady state operation at high plasma pressures for advanced tokamaks. Indeed, for an advanced scenario in ITER, the normalized plasma pressure $\beta_N \equiv \beta(\%)/[I(MA)\ /a(m)B(T)]$ can be increased from about 2.5 (no-wall beta limit) to about 3.5 (ideal-wall limit), if the RWM is stabilized [1].

Both JET RWM experiments and simulations using the stability code MARS-F aim at understanding physics of the RWM. From the modeling point of view, the key issue is the choice of adequate damping models, that are used in the MARS-F code. The correct prediction of experimental results depends sensitively on the damping models [2]. Therefore, a key purpose of RWM experiments is to benchmark different models, that then lead to better understanding of the RWM physics.

Two types of experiments on JET are modeled. The first is the minimal (critical) plasma toroidal rotation speed needed in order to stabilize the mode. The second is the resonant field amplification (RFA) experiments, which can be viewed as the MHD spectroscopy for the RWM. In this paper only the $n = 1$ RWM is studied.

2. Damping models

At least two types of dissipation play important roles in the stabilization of RWM by plasma rotation. One comes from the Alfvénic resonances ("Afvén continuum damping") that is described by ideal MHD.

The other dissipation comes from ion Landau damping for the ion motion along the field lines. This kinetic effect is modeled as additional terms in MHD equations in the MARS-F code. In the simplest form a parallel viscosity term is introduced as

$$\vec{F}_{\rm visc} = -\kappa_{||}|k_{||}|v_{th,i}\rho\vec{v}_{||}$$

that represents the parallel sound wave damping, with a free parameter $\kappa_{||}$ for the model. We also implemented a more physics-based semi-kinetic damping model where the damping force is computed from the imaginary part of the kinetic energy perturbation, calculated for a cylindrical plasma [3].

3. Resonant field amplification

A. Geometry and equilibrium

In JET RFA experiments, the error fields are produced by currents flowing in the internal saddle coils or in the error field correction coils (EFCC). Figure 1 shows the geometry for the MARS-F modeling of RFA experiments. The JET wall is modeled as a complete thin shell. Both internal saddles and EFCC are modeled as large enough number of coils along the toroidal direction, that produce an

$\exp(jn\phi)$ dependence of the current density along the ϕ angle. The radial and poloidal locations of the saddle and pick-up coils are the same as in the experiments. We also include a thin shell with a poloidal gap in the outboard mid-plane (dashed line in Fig. 1), in order to represent the effect of 3D conducting structures located in JET between the EFCC and the pick-up coils. Without the second shell, it is not possible to reproduce the RFA experiments with EFCC and AC excitation currents.

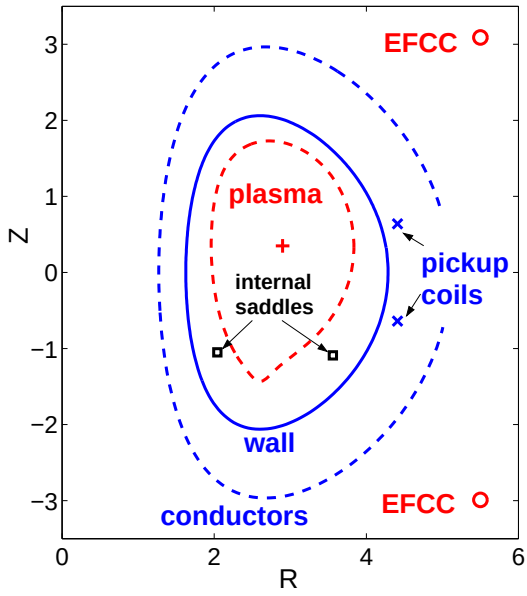

Figure 1: *Geometry of RFA experiments on JET with internal saddle coils (squares) and EFCC (circles). The JET 3D conducting structures are modeled as a 2D wall with a poloidal gap (dashed line between the pick-up coils and the EFCC).*

We chose an equilibrium reconstructed from the JET shot 62024. The toroidal vacuum field is about 1.2T, and the total plasma current is about 1.0MA. The plasma has rather broad current profile, with the internal inductance $l_i = 0.73$. The computed β_N limits are 2.63 without the wall and 3.36 with the ideal JET wall.

B. RFA with internal saddles

First results are shown for RFA experiments where the error field is produced by a DC current in the saddle coils. We compared both the amplitude and the phase of the amplification factor, and found that the code can reproduce the experimental results only if a strong sound wave damping or the semi-kinetic damping is included. In all the RFA simulations, we chose the semi-kinetic damping model. The RWM in JET is also excited by standing waves launched by the saddle coils. Two flux signals are measured: one is in phase (toroidally) with the saddle coils (denoted here as $B_r(0\,\mathrm{deg})$), the other is in 90^o toroidal phase shift with the saddles ($B_r(90\,\mathrm{deg})$). In MARS-F simulations, we launch traveling waves. The plasma responses from two traveling waves, with the same frequency but opposite toroidal directions, are then combined to obtain the response for a standing wave. Traveling waves give more rich information about the plasma response.

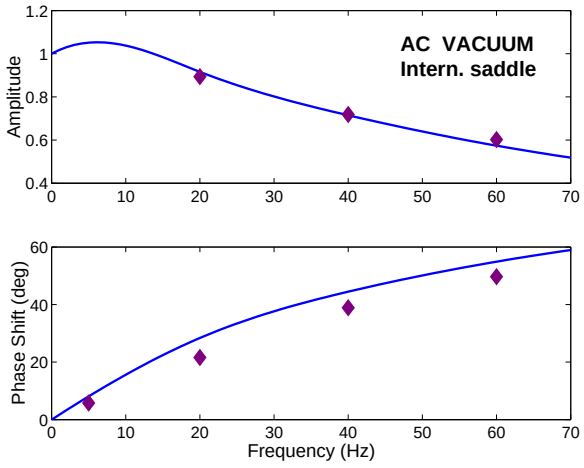

Figure 2: *Comparison of JET data (dots) from vacuum shots with MARS-F results (curves) for internal saddle coils with standing waves.*

Figure 2 shows the comparison of the JET vacuum shots (i.e. with only the saddles and walls but no plasma) and the MARS-F modeling. Plotted are the amplitude (normalized by the value at zero frequency) of the sensor flux ($B_r(0\,\mathrm{deg})$ in this case), and the temporal phase lag of the signal with respect to the excitation current. A good fit to the experimental data is obtained by MARS-F. The

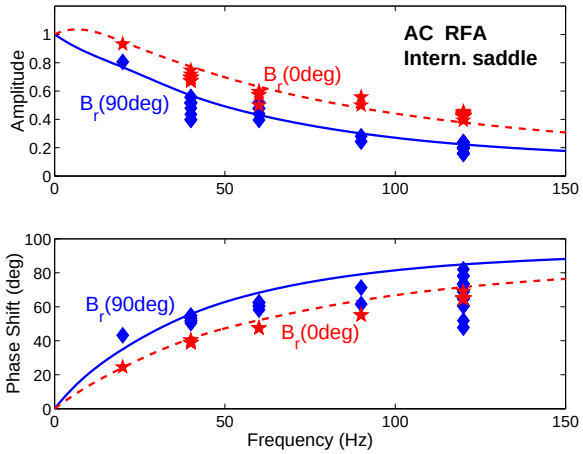

Figure 3: *Comparison of JET data (dots) from RFA experiments with MARS-F results (curves) for internal saddle coils with standing waves.*

similar comparison is made for the RFA experiments (with all the components including the plasma), as shown in Fig. 3 for a wide frequency range from 0 to 120Hz. The agreement between MARS-F modeling and the experiments is reasonable for both amplitude and the temporal phase shift.

The plasma response to an AC external field can be described by a frequency dependent transfer function, in a similar way as we have done for the feedback control of the RWM [4]. We define a function

$$P(j\omega) = \frac{\psi(\omega)}{\psi(\omega = 0|\text{vacuum})},$$

where $\psi(\omega)$ is the total flux through the pick-up coils and depends on the excitation frequency ω. The plasma response to a traveling wave is completely described by $P(j\omega)$. The plasma response to a standing wave can be easily constructed from $P(j\omega)$.

The transfer functions for the vacuum and the RFA shots with internal saddle coils are computed by MARS-F and represented by 2-pole Padé approximation

$$P_{\text{int}}^{\text{vac}}(j\omega) = \frac{0.77}{j\omega + 1.0} + \frac{0.071}{j\omega + 0.31},$$

$$P_{\text{int}}^{\text{RFA}}(j\omega) = \frac{1.00 + 0.54j}{j\omega + 0.72 - 0.21j} + \frac{-0.029 - 0.017j}{j\omega + 0.22 - 0.48j},$$

where ω is normalized by the wall time of the JET wall.

C. RFA with EFCC

The RFA experiments with EFCC are also modeled by MARS-F. We found that it is easy for MARS-F to recover the plasma response to the static error fields. However, for the time-varying fields, in order to match the data from vacuum shots, we have to introduce a second shell with a poloidal gap, as shown in Fig. 1, and adjust the radial position, the poloidal extent of the gap, as well as the wall time for the second shell. The best fit to the experimental data, as shown in Fig. 4, corresponds to a thin shell placed at $r = 1.7a$ (a is the plasma minor radius), with poloidal gap covering about 10% of the total poloidal circumference, and with the wall time 10 times larger than the JET wall time. The resistivity in the poloidal gap is 100 times larger than the other region. It should be noted that once these parameters for the second shell have been fixed in the vacuum matching, the same shell is used consistently in all the other modelings, including those shown in Fig. 2, 3, 5. No extra scaling factors have been introduced. Fig.

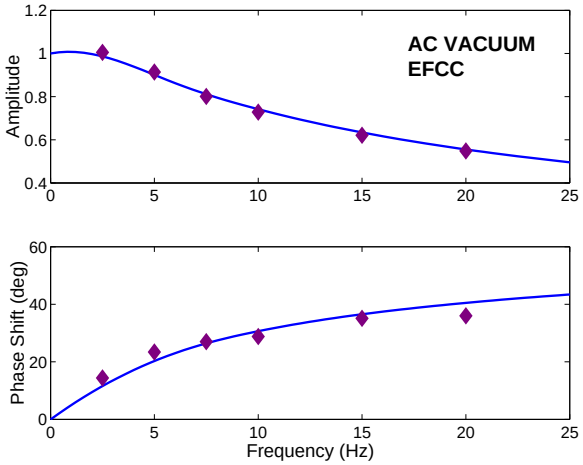

Figure 4: *Comparison of JET data (dots) from vacuum shots with MARS-F results (curves) for EFCC with standing waves.*

5 shows the comparison of the RFA experimental data with the MARS-F calculations for EFCC. The experimental data are rather scattered due to the variation of the plasma

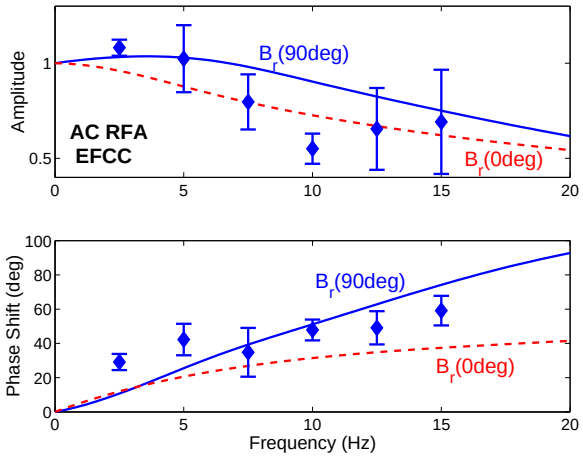

Figure 5: *Comparison of JET data (dots) from RFA experiments with MARS-F results (curves) for EFCC with standing waves.*

conditions (e.g. the plasma pressure), as well as the fact that the $B_r(90\,\mathrm{deg})$ is rather weak compared with $B_r(0\,\mathrm{deg})$ which is dominated by the vacuum field. By the latter reason we show the experimental data only for the $B_r(90\,\mathrm{deg})$ signal.

The transfer functions with EFCC are computed as

$$P^{\mathrm{vac}}_{\mathrm{EFCC}}(j\omega) = \frac{0.37}{j\omega+1.0} + \frac{0.10}{j\omega+0.16},$$
$$P^{\mathrm{RFA}}_{\mathrm{EFCC}}(j\omega) = \frac{0.35-0.018j}{j\omega+0.88-0.009j} + \frac{0.11+0.012j}{j\omega+0.16+0.007j}.$$

4. Critical plasma rotation

We computed the critical plasma rotation speed versus a parameter C_β defined as $C_\beta \equiv (\beta_N - \beta_N^{\mathrm{no-wall}})/(\beta_N^{\mathrm{ideal-wall}} - \beta_N^{\mathrm{no-wall}})$, using different damping models as shown in Fig. 6. The sound wave damping model predicts different critical rotation speed depending on the choice of $\kappa_\parallel$. Generally there is no strong dependence of critical rotation on the plasma pressure. For the JET plasma, the predicted critical rotation speed at the $q = 2$ surface is about 0.5% of the toroidal Alfvén speed v_A. Initial analysis of the JET data shows critical velocities consistent with the kinetic model, indicating that the RWM is normally strongly damped in JET. [The typical plasma rotation speed in JET is much higher, e.g. about 1.7%v_A at $q = 2$ for the shot considered here.]

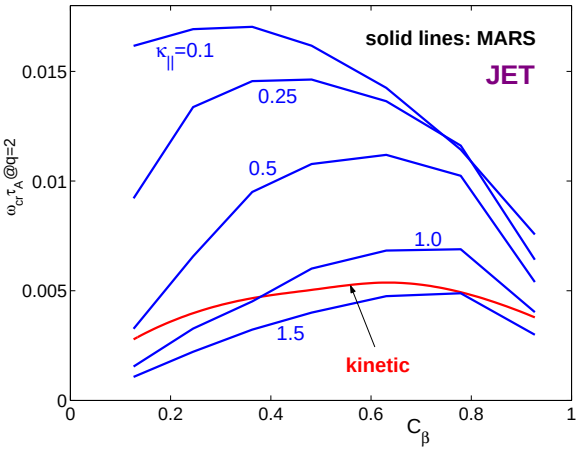

Figure 6: *Critical plasma rotation, measured at the $q = 2$ surface, required to make the RWM marginally stable. MARS-F computations (solid lines) with different damping models are compared with the JET experimental data (filled diamonds).*

5. Conclusion

Using the MARS-F code, we were able to model the JET RWM experiments, for both the critical plasma rotation required for the RWM stabilization, and the resonant field amplification. The semi-kinetic damping model gives adequate predictions for both critical rotation and RFA. For the RFA experiments in JET, it is important to take into account the influence of the conducting structures between the EFCC and the pick-up coils. We model these structures by a partial wall with poloidal gap. The plasma responses in the RFA experiments are computed as 2-pole Padé approximations. This study allows RWM stability in ITER to be predicted with better confidence than previously possible.

Work performed under the European Fusion Development Agreement.

[1] Y.Q. Liu, et al, Nucl. Fusion **44** 232 (2004).
[2] A. Bondeson, et al, Plasma Phys. Controll. Fusion **45** A253 (2003).
[3] A. Bondeson and M.S. Chu, Phys. Plasmas **3** 3013 (1996).
[4] Y.Q. Liu, et al, Phys. Plasmas **7**, 3681 (2000).